PSFC/JA-06-45

The effect of sheared axial flow on the interchange mode in a hard-core Z-pinch

[1]A. Kouznetsov, [2]J.P. Freidberg, and [3]J. Kesner

[1,2,3]MIT Plasma Science and Fusion Center, 167 Albany Street, Cambridge, MA 02139, USA

This work was supported by the U.S. Department of Energy, Grant No. DE-FG02-91ER-54109

Submitted for publication in the Physics of Plasma (Janaury 2006)

The effect of sheared axial flow on the interchange mode in a hard-core Z-pinch

A. Kouznetsov, J.P. Freidberg, and J. Kesner

Plasma Science and Fusion Center, Massachusetts Institute of Technology,

Cambridge, Massachusetts, 02139

Abstract

It is well known that a static (i.e. $\mathbf{v} = 0$) closed field line configuration, such as a levitated dipole, or a hard-core Z-pinch, can be stabilized against ideal MHD interchange modes when the edge pressure gradient is sufficiently weak. The stabilizing effect is provided by plasma compressibility. However, many laboratory plasmas exhibit a sheared velocity flow, (i.e. $\mathbf{n} \cdot \nabla \mathbf{v} \neq 0$), and this flow may affect the marginal stability boundary. The present work addresses this issue by an analysis of the effect of axially sheared flow on interchange stability in a hard-core Z-pinch, a cylindrical model for the levitated dipole configuration. Specifically, the goal is to learn whether sheared flow is favorable, unfavorable, or neutral with respect to MHD stability. Analytic calculations of marginal stability for several idealistic velocity profiles show that all three options are possible depending on the shape of the shear profile. This variability reflects the competition between the destabilizing Kelvin-Helmholtz effect and the fact that shear makes it more difficult for interchange perturbations to form. Numerical calculation are also presented for more realistic experimental profiles and compared with the results for the idealized analytic profiles.

I. Introduction

The goal of this paper is to theoretically investigate the effect of sheared axial flow on the MHD stability of a closed line configuration. The primary experimental application of the analysis is to the levitated dipole experiment (LDX) [1,2]. The motivation is as follows. The toroidal LDX configuration can be modeled theoretically as a cylindrical hardcore Z-pinch. It is well known [3] that a simple Z-pinch without an equilibrium flow (i.e. $\mathbf{v} = 0$) is potentially unstable to two MHD modes - the $m = 1$ helical mode and the $m = 0$ interchange mode. The hardcore stabilizes the $m = 1$ mode. In a closed line configuration the $m = 0$ interchange mode (i.e. the sausage instability) can be stabilized by a sufficiently weak pressure gradient near the edge of the column. The maximum allowable pressure gradient directly sets the β limit of the plasma, whose value is critical to the ultimate viability of the concept.

However, many laboratory plasmas exhibit a substantial equilibrium sheared velocity flow, (i.e. $\mathbf{n} \cdot \nabla \mathbf{v} \neq 0$). This flow may affect the $m = 0$ marginal stability boundary, and hence the maximum value of β. The present work directly addresses this issue by an analysis of the effect of axially sheared flow on the ideal MHD stability limit of the $m = 0$ mode in a hardcore Z-pinch. Specifically, the goal is to learn whether sheared flow is favorable, unfavorable, or neutral with respect to MHD stability. Analytic calculations of marginal stability for several idealistic velocity profiles in the slab limit show that all three options are possible depending on the shape of the shear profile. This variability reflects the competition between the destabilizing Kelvin-Hemholtz effect and the fact that shear makes it more difficult for interchange perturbations to form at short

wavelengths. Numerical calculation are presented for more realistic experimental profiles and compared with the results for the idealized analytic profiles. The numerical results are also used to predict the change in critical β due to realistic velocity shear profiles.

The effects of flow on MHD stability have been studied for many years and as such it is useful to review some of the most relevant studies to put the present work in perspective. As is well know the highly desirable property of self-adjointness in the linear stability equations vanishes when flow is included [4]. This has caused a large part of the effort to focus on simple geometries such as a slab or cylinder. Even then, the resulting problems remain quite complicated mathematically, often requiring numerical solutions for the eigenvalues and eigenfunctions.

Some early studies involved the effect of rotation on a pure θ-pinch. Taylor [5] showed that centrifugal effects could drive rotational instabilities for $m \geq 2$ modes for $k_{\|} = 0$, presumably the worst mode in terms of minimizing the stabilizing effects of line bending. Freidberg and Wesson [6] showed the counter-intuitive result that $m = 1$ could also be driven unstable, but only for a finite, non-zero value of $k_{\|}$. This unexpected result arose from the non-self adjointness of the MHD force operator. A similar situation arises in the present work.

Several authors have investigated the effect of sheared axial flow on a general screw pinch. Bondeson, Iacono and Bhattacharjee [7] studied the effects of flows on the Suydam criterion. They found that the flow decreases the maximum stable pressure gradient. E. Hameri [8] came to the similar conclusions using analytical approximations.

The effect of toroidal rotation on the stability of ballooning modes was considered by E. Hameri and P. Laurences [9] in mid the mid-80s. They found that the toroidal rotation

had a destabilizing effect on the plasma β limit . However, ideal ballooning modes are of limited interest to LDX because of the absence of magnetic shear [10,11]. They do not exist in a cylindrical Z-pinch.

Recent interest in Z-pinch plasmas has led to several numerical studies of the stability of plasmas with sheared flows. V. Sotnikov et al [12] and Zhang and Ding [13] showed that supersonic flows could decrease the growth rate of macroscopic perturbations. Also, partial stabilization of the plasma column by axial sheared flows was reported by Desouza-Machado, Hassam and Ramin Sina[14]. The Rayleigh-Taylor instability, a close analog of the interchange instability, has also been of interest to the geophysics community. Kuo [15] in 1963 and Guzdar et. al.[16] in 1982 found that velocity shear decreases the growth rate of the Rayleigh-Taylor mode and showed that unlike the static case, the most unstable wavenumber is finite. An analytic slab geometry calculation carried out by A.Hassam[17] demonstrated that velocity shear decreases the growth rate of the Rayleigh-Taylor instability and non-linearly positively stabilizes marginally stable profiles. In a similar calculation Hassam [18] also showed that for the short wavelength interchange mode in an elongated plasma, sheared flows stabilize the plasma.

At the same time the introduction of sheared flows may give rise to KH (Kelvin-Helmholtz) instability [19]. Experimental observations and the relative importance of the KH mode vs. flow shear stabilization near a plasma limiter were reported by Brochard et al [20]. Many previous studies, often motivated by short-lived Z-pinches, typically concentrated on the effect of sheared flows on highly unstable plasma profiles, but did not consider the effect of an axial flow on weakly unstable or marginally stable plasma pressure profiles.

The net result is that while considerable progress has been made, at the present time there is no clear and unique understanding of whether or not an axial sheared flow would be favorable, unfavorable, or neutral with respect to the important question of β limits in a hardcore Z-pinch, modeling the LDX configuration. This is the main objective of the present paper.

The paper is organized as follows: In Section 2 the standard second order radial eigenvalue equation for the m = 0 interchange mode in a static Z-pinch is modified to include non-zero axial flows. In Section 3 we consider the slab limit of the LDX configuration. Section 4 presents an analytical derivation of new local stability criteria for several idealistic velocity shear profiles. In section 5 we return to the cylindrical geometry and present numerical calculations, which determine the stability boundaries using more realistic experimental profiles for the plasma pressure and the flow velocity.

II. Eigenmode equation for a general Z-pinch with an axial flow

This section discusses the eigenvalue equation for a cylindrical screw pinch configuration, including an axial flow. The starting point is the ideal MHD model

$$\begin{aligned}
&\frac{\partial \rho}{\partial t} + \nabla \cdot (\rho \mathbf{v}) = 0 \\
&\rho\left(\frac{\partial \mathbf{v}}{\partial t} + \mathbf{v}\cdot\nabla\mathbf{v}\right) = \mathbf{J}\times\mathbf{B} - \nabla p \\
&\frac{d}{dt}\left(\frac{p}{\rho^{\gamma}}\right) = 0 \\
&\nabla\times\mathbf{B} = \mu_0\mathbf{J} \\
&\frac{\partial \mathbf{B}}{\partial t} = \nabla\times(\mathbf{v}\times\mathbf{B})
\end{aligned} \tag{1}$$

The non-trivial quantities entering the analysis are as follows: the pressure $p = p_0 + p_1$, the magnetic field $\mathbf{B} = B_{0\theta}\mathbf{e}_\theta + B_{0z}\mathbf{e}_z + \mathbf{B_1}$, and the axial velocity

$\mathbf{v} = V_0 \mathbf{e}_z + \mathbf{v_1}$. Here all equilibrium quantities are functions only of r [i.e. $Q_0 = Q_0(r)$] and all perturbed quantities have the standard normal mode dependence $Q_1 = Q_1(r) \exp\left[i\left(-\omega t + m\theta + kz\right)\right]$. For simplicity the "zero" subscript is hereafter suppressed on all equilibrium quantities. Note that with an axial flow the eigenvalue ω is in general complex. The next step is to introduce the displacement vector $\boldsymbol{\xi}$, defined as $\mathbf{v}_1 = -i\omega\boldsymbol{\xi} + \mathbf{V}\cdot\nabla\boldsymbol{\xi} - \boldsymbol{\xi}\cdot\nabla\mathbf{V}$. Following the usual MHD stability procedure [21] it is straightforward to show that the full eigenmode equation for the general screw pinch in the presence of an axial flow has exactly the same form as without flow if we make the formal substitution $\omega \to \omega - kV(r)$.

The general eigenvalue equation reduces considerably for interchange modes in a hard-core Z-pinch. The simplified equation is obtained by setting $B_z(r) = 0$ and $m = 0$. Also, further simplification arises by making the well satisfied approximation that the unstable eigenvalues of interest are much smaller in magnitude than the compressional Alfven frequency: $|\omega| \ll kV_A$. Under these assumptions the final eigenmode equation is given by

$$\frac{d}{dr}\left[\frac{\rho}{k^2 r}\left(\omega - kV\right)^2 \frac{d\psi}{dr}\right] + \frac{\rho}{r}\left[\omega_S^2 K - \left(\omega - kV\right)^2\right]\psi = 0 \tag{2}$$

where $\omega_S^2(r) = 2V_s^2 / r^2$, $V_S^2(r) = \gamma p / \rho$ is the square of the adiabatic sound speed,

$$K(r) = \frac{rp'}{\gamma p} + \frac{2B_\theta^2}{B_\theta^2 + \gamma\mu_0 p} \tag{3}$$

is the Kadomtsev stability function [3] and $\psi = r\xi_r(r)$ is proportional the radial component of the perturbation. Kadomtsev showed that $K(r) > 0$ is a necessary and

sufficient local stability criterion against the $m = 0$ interchange mode for static equilibrium.

The appropriate boundary conditions on Eq. (3) require that the function ψ vanish at the plasma boundaries.

$$\psi(r_c) = \psi(r_w) = 0 \tag{4}$$

Here, r_c is the radius of the hard core and r_w is the radius of the outer shell. See Fig.1. The usual experimental situation has $r_w \gg r_c$.

The normal mode approach requires solving equation (2) subject to the boundary conditions given by Eq. (4) for given plasma and velocity profiles. The full solution for arbitrary profiles can only be found numerically.

This section closes with an interesting suggestive, but misleading intuition, about the effect of flow on stability resulting from a quadratic integral relation obtained by multiplying Eq. (2) by $\psi*$ and averaging over the plasma volume. The requirements that both real and imaginary parts vanish yield the following expression for the growth rate ω_i: $\omega_i^2 = -\langle \omega_s^2 K \rangle_0 + \langle k^2 V^2 \rangle_1 - \langle kV \rangle_1^2$. Here

$$\langle Q \rangle_n = \frac{\int Q(\rho/r)\left(n|\psi'|^2 + k^2|\psi|^2\right)dr}{\int (\rho/r)\left(|\psi'|^2 + k^2|\psi|^2\right)dr} \tag{5}$$

Clearly the condition for stability is given by

$$\langle \omega_s^2 K \rangle_0 \geq \langle k^2 V^2 \rangle_1 - \langle kV \rangle_1^2 \tag{6}$$

Note that for uniform or zero axial flow the right hand side of Eq. (6) vanishes and the stability criterion reduces to that given by Kadomtsev. When there is shear in the flow, Schwartz's inequality implies that the right hand side is always positive. The

implication would seem to be that it is now more difficult to achieve stability and therefore flow shear is always destabilizing. This conclusion is not correct for the following reason. Since the problem is not self-adjoint the Energy Principle does not apply. Thus, while substituting the eigenfunction for the static case into Eq. (6) as a trial function suggests a more unstable situation, there is no guarantee that the actual eigenvalue is always approached from the stable side of the spectrum. In fact, in certain important examples discussed shortly it is found that just the opposite occurs, demonstrating that velocity shear can be a stabilizing effect in spite of misleading intuition generated by Eq. (6).

In the next chapter we derive a slab geometry approximation that leads to an analytically solvable equation.

III. The slab geometry model

The counter intuitive effect just described as well as a more general view of the effects of flow shear can be obtained by taking a simple slab limit of the eigenvalue equation, which allows an analytic solution. The slab limit is somewhat artificial with respect to the actual experimental situation in LDX but still makes good sense physically. The limit is obtained by assuming the hard core radius and outer boundary surface are close to one another so that the plasma resembles a thin shell. Specifically, we assume that $(r_w - r_c)/(r_w + r_c) \ll 1$. We then expand $r = r_0 + x$ where $r_0 = (r_c + r_w)/2$. The range of the new independent variable x is defined by $-a \le x \le a$ where $a = (r_w - r_c)/2$ and $a \ll r_0$. The eigenvalue equation reduces to

$$\frac{d}{dx}\left[\left(V_p - V\right)^2 \frac{d\psi}{dx}\right] + \left[\omega_S^2 K - k^2\left(V_p - V\right)^2\right]\psi = 0 \qquad (7)$$

where $V_p = \omega / k$ is the phase velocity, $\omega_S^2 = \omega_S^2(r_0) = 2V_S^2(r_0)/r_0^2$ and

$V = V(x), K = K(x)$ are the spatially varying velocity and Kadomtsev profiles.

Introducing $\psi(x) = U(x)/(V - V_p)$, leads to the final desired form of the slab eigenvalue equation:

$$U'' - \left[k^2 - \frac{\omega_S^2 K}{(V - V_P)^2} + \frac{V''}{V - V_p} \right] U = 0 \qquad (8)$$

In the next chapter this equation is solved analytically for several idealistic velocity profiles to determine the effect of sheared axial flow on marginal stability.

IV. Marginal stability for the slab model

Equation (8) can be solved analytically for a variety of profiles consisting of constant and linear velocity segments. The case of a purely constant velocity is uninteresting. It does not change the self-adjointness of the MHD force operator and the stability analysis immediately reduces to that of the static case by the introduction of a Doppler shifted frequency.

The more interesting cases considered treat three specific velocity profiles, each with axial shear: (a) a constant shear velocity profile, (b) a triangle-shaped velocity profile with velocity shear positive in one region and negative in the other and (c) an "S" shaped profile where the shear is constant in a narrow region and connects to constant velocity regions at each edge with equal but opposite sign velocities. For each of these models the full dispersion relation is derived leading to a determination of the marginal stability criterion.

A. The case of constant velocity shear.

This configuration models the situation where the Kadomtsev function is negative (i.e. $K < 0$) over a narrow region of the plasma (i.e. is destabilizing) and the velocity shear is a smooth function over this region. An illustration of the smooth cylindrical profiles and the corresponding slab approximation is shown in Fig. 2.

The slab model is further simplified by assuming that $-K_{\max} / K_{\min} \gg 1$ with $K_{\max} > 0$ and $K_{\min} < 0$. In this limit the outer solutions in the regions $L < |x| < a$ decay very rapidly, a behavior that is accurately approximated by modifying the boundary conditions such that $\psi(-L) = \psi(L) = 0$ where $L^2 \approx -K_{\min} / K''_{\min}$. As is shown shortly the marginal stability boundary is independent of L. For this model we assume that in the region $0 < |x| < L$ the Kadomtsev function is a constant, $K(x) = K_{\min} < 0$, and the velocity profile is smooth, $V(x) = V'(0)x = V'x$. Under these assumptions the eigenvalue equation reduces to

$$U'' - \left[k^2 - \frac{\omega_S^2 K_{\min}}{(V'x - V_P)^2} \right] U = 0 \tag{9}$$

The general solution is easily found in terms of modified Bessel functions and is given by $U(z) = z^{1/2} \left[\hat{C}_1 K_\nu(z) + \hat{C}_2 I_\nu(z) \right]$ or in terms of ψ

$$\psi(z) = z^{-1/2} \left[C_1 K_\nu(z) + C_2 I_\nu(z) \right] \tag{10}$$

Here $z = kx - \omega / V'$ is a complex coordinate and the order ν is a function of $K_{\min}$:

$$\nu = \sqrt{\frac{1}{4} - \frac{\omega_S^2 K_{\min}}{V'^2}} \tag{11}$$

The boundary conditions lead to a simple dispersion relation:

$$\det\begin{vmatrix} I_\nu(z_+) & K_\nu(z_+) \\ I_\nu(z_-) & K_\nu(z_-) \end{vmatrix} = 0 \tag{12}$$

where $z_\pm = \pm kL - \omega / V'$

The eigenvalue ω as a function of wave number k is illustrated in Fig. 3 for a typical unstable case, $\nu = 3/2$. For this value the Bessel functions reduce to simple exponentials and algebraic terms from which the dispersion relation reduces to

$$\frac{\omega}{\omega_S} = i\left[\kappa \coth(2\kappa) - \frac{\kappa^2 + 1}{2}\right]^{1/2} \left(-K_{\min}\right)^{1/2} \tag{13}$$

where $\kappa = kL$. Also shown the growth rate curve for the static case $V' = 0$ whose growth rate is given by

$$\frac{\omega}{\omega_S} = i\frac{\kappa}{\left(\kappa^2 + \pi^2/4\right)^{1/2}} \left(-K_{\min}\right)^{1/2} \tag{14}$$

Observe that the growth rate of the mode with a sheared flow increases with *k* starting at the origin, reaches a maximum, and finally decreases to zero at the maximum stable wave number $k = k_{\max}$. As ν decreases towards the value unity (corresponding to $K_{\min}$ increasing from the negative direction) the region of unstable wave numbers shrinks to zero; that is $k_{\max} \to 0$ as $\nu \to 1$.

The marginal stability boundary can be found analytically [22] by focusing attention on the behavior of the dispersion relation for small kL. Specifically, we write $\omega = \omega_r + i\omega_i$, expand $\nu = 1 + \delta\nu$, and assume the following ordering scheme: $\omega_i / V' \ll kL \ll \delta\nu \ll 1$. Also $\omega_r = 0$ by symmetry. Under these assumptions the small argument expansion of the Bessel functions can be used and the dispersion relation reduces to

$$\omega = \frac{i\pi}{2}\left(-\frac{K_{\min}}{K''_{\min}}\right)^{1/2} kV'(\nu - 1) \tag{15}$$

Note that for $\nu > 1$, there always exists an exponentially growing solution to the eigenmode equation. After a transformation of variables, it can be shown that this result overlaps with the early result of Kuo [15] who was interested in the geophysical problem of Rayleigh-Taylor instabilities in stratified fluids.

The conclusion is that a constant shear flow has a stabilizing effect on the interchange mode. The intuition is that flow shear inhibits the ability of the plasma to form very short wavelength instabilities, which are the most unstable modes for the case without flow. Specifically, the marginal stability boundary $K_{\min} \geq 0$ for the case of zero flow relaxes to $K_{\min} \geq -(3/4)V'^2/\omega_S^2$ for a constant shear flow. In terms of the physical variables the modified stability criterion can be written as

$$\frac{rp'}{\gamma p} + \frac{2B_\theta^2}{B_\theta^2 + \gamma\mu_0 p} > -\frac{3}{4}\frac{V'^2}{\omega_S^2} \tag{16}$$

When the flow velocities become comparable to the sound speed then the stability modifications become substantial.

B. The case of a velocity profile with no-slip boundary conditions

The situation modeled here corresponds to a plasma confined between rigid boundary surfaces with no-slip boundary conditions at each surface. Sketches of the actual cylindrical problem and the slab approximation are illustrated in Fig.4. Note that we again assume that $K_{\min} < 0$. The axial velocity profile is similar to that of a liquid flowing between two pipes of different radii.

The solution to the eigenvalue problem can be simplified by noting that the velocity has even symmetry: $V(x)=V(-x)$. This implies that the eigenfunctions are either purely even or purely odd. The most unstable case corresponds to an eigenfunction with no radial nodes. Therefore, the appropriate boundary conditions on ψ can be written as $\psi'(0)=0$ and $\psi(a)=0$. Since the shear in the region $0\le x\le a$ is constant the solution can again be written as a sum of Bessel functions: $\psi(z)=z^{-1/2}\left[C_1K_\nu(z)+C_2I_\nu(z)\right]$. Here, $z=k(a-x)-\omega/V'$ with $V'>0$ and ν is again given by Eq. (11). Applying the boundary conditions leads to the following dispersion relation

$$\det\begin{vmatrix}\left[I_\nu(z_0)/z_0^{1/2}\right]' & \left[K_\nu(z_0)/z_0^{1/2}\right]' \\ I_\nu(z_a) & K_\nu(z_a)\end{vmatrix}=0 \tag{17}$$

where $z_0=z(0)=ka-\omega/V'$ and $z_a=z(a)=-\omega/V'$.

The qualitative properties of the instability can be obtained by examining the dispersion relation for the unstable case $\nu=3/2$. For this case the dispersion relation reduces to a third order polynomial in the variable $\Omega=\omega/V'-ka$ given by

$$\Omega^3+(\kappa+\tanh\kappa)\Omega^2+2\kappa\Omega+2(\kappa-\tanh\kappa)=0 \tag{18}$$

where $\kappa=ka$. The real and imaginary parts of the Doppler shifted frequency are plotted in Fig. 5. Note that in this case the mode is unstable even as $ka\to\infty$. In fact the $ka\to\infty$ limiting value of the unstable eigenfrequency is easily found and can be written as

$$\frac{\omega}{V'}-ka=1+i \tag{19}$$

Further numerical studies show that instability persists until ν decreases to its marginal value $\nu = 1/2$. The marginal stability boundary can also be found analytically [22] by focusing on the region of small ka. Applying the ordering scheme $\omega_i / V' \ll ka \ll \delta\nu \ll 1$ and using the small argument expansion of the Bessel functions leads to

$$\frac{\omega}{V'} = ka\,\delta\nu\left[1 + i\frac{\pi}{2}\left(\delta\nu + |\delta\nu|\right)\right] \tag{20}$$

where $\nu = 1/2 + \delta\nu$. For $\nu > 1/2$ there is always an unstable solution. The marginal stability limit $\nu = 1/2$ corresponds to the value $K_{\min} = 0$. In other words a no-slip velocity flow does not affect the stability boundary, which reduces to the original Kadomtsev stability limit

$$\frac{rp'}{\gamma p} + \frac{2B_\theta^2}{B_\theta^2 + \gamma\mu_0 p} > 0 \tag{21}$$

The physical explanation for this behavior is as follows. In the limit of zero flow the unstable eigenfunctions tend to be localized in the region where $K = K_{\min} < 0$. With a no-slip velocity flow of the type considered here there is by definition always a region where $V' = 0$. If $K_{\min} < 0$ in this region then localized modes will not feel the stabilizing effects of velocity shear and the stability boundary reduces to the no-flow limit.

C. The case of a counter-streaming velocity profile

The last model of interest involves a flow pattern consisting of two regions of plasma counter-streaming with respect to one another. The regions are connected by a thin of layer of plasma with a constant shear profile. The profiles for the cylindrical geometry and slab approximation are illustrated in Fig. 6. Because the flow pattern has an "S-like"

shape the second derivative changes sign somewhere in the plasma suggesting that the Kelvin-Helmholtz instability may be excited.

The analysis of this configuration is similar to case (A). The main difference is that the boundary conditions at $x = \pm L$ must be modified as follows. In the constant velocity regions $L \le |x| \le a$ the solution to the eigenvalue equation reduces to simple exponential functions: $\exp(\pm\alpha k x)$ where $\alpha^2 = 1 - \omega_S^2 K_{\min} / (\omega - kV'L)^2$. The perturbed displacement is again required to vanish at $x = \pm a$. The solutions in these regions reduce to $\psi(\pm x) = C_\pm \sinh\left[\alpha k (x \mp a)\right]$, leading to boundary conditions at $x = \pm L$ given by $\psi'(\pm L) \pm \alpha k \coth\left[\alpha k (a - L)\right]\psi(\pm L) = 0$ where 'prime' denotes x differentiation.

In the region of sheared flow the solutions again reduce to Bessel functions: $\psi(z) = z^{-1/2}\left[C_1 K_\nu(z) + C_2 I_\nu(z)\right]$, where as before $z = kx - \omega / V'$. For the interesting regime corresponding to a thin shear layer we assume that $kL \sim 1$ and $L \ll a$. Applying the boundary conditions then leads to the following dispersion relation.

$$\det \begin{vmatrix} \left[z_+^{-1/2} e^{\alpha z_+} I_\nu(z_+)\right]' & \left[z_+^{-1/2} e^{\alpha z_+} K_\nu(z_+)\right]' \\ \left[z_-^{-1/2} e^{-\alpha z_-} I_\nu(z_-)\right]' & \left[z_-^{-1/2} e^{-\alpha z_-} K_\nu(z_-)\right]' \end{vmatrix} = 0 \qquad (22)$$

where $z_\pm = \pm kL - \omega / V'$ and 'prime' now denotes z differentiation.

The dispersion relation for a typical unstable case corresponding to $\nu = 1/2$ is illustrated in Fig. 7. Note that this value of ν is equivalent to $K_{\min} = 0$ so that the instability is a pure fluid dynamics mode, not dependent on plasma physics. Observe that

the mode is unstable for a finite range of wave numbers $k_{\min} < k < k_{\max}$. The values of $k_{\min}$ and $k_{\max}$ are easily found by solving the dispersion relation which reduces to the following simple analytic form

$$\frac{\omega}{V'} = i\left[\left(\kappa - \frac{1}{2}\right)^2 - \frac{1}{4}\exp(-4\kappa)\right]^{1/2} \tag{23}$$

with $\kappa = kL$. We find that the critical wave numbers are given by $k_{\min} = 0$ and $k_{\max} \approx 0.64$. Also, by symmetry, $\mathrm{Re}(\omega) = 0$.

As the value of ν decreases the system remains unstable, although the two critical values of k start to coalesce. Eventually, when ν decreases below a critical value, $k_{\min}$ and $k_{\max}$ overlap. This corresponds to the marginal stability point of the system. Numerically, marginal stability occurs when $\nu = 0$ at the fully coalesced value of wave number $kL \approx 0.60$. This result can be verified analytically by setting $\omega = 0$ and $\nu = 0$ in the dispersion relation. The result, after a short calculation, is a transcendental equation for the marginal κ that can be written as

$$\frac{\kappa I_0'(\kappa)}{I_0(\kappa)} = \frac{1}{2} - \left(\kappa^2 - \frac{1}{4}\right)^{1/2} \tag{24}$$

It has a single real solution for κ given by $\kappa \approx 0.60$ thereby confirming the numerical results.

Observe that the marginal stability condition $\nu = 0$ corresponds to $K_{\min} = V'^2/4\omega_S^2$. As compared to the case of no flow, the value of $K_{\min}$ has increased from zero to a positive value; that is the system is more unstable. In terms of the physical variables the stability condition has the form

$$\frac{rp'}{\gamma p}+\frac{2B_\theta^2}{B_\theta^2+\gamma\mu_0 p}>\frac{1}{4}\frac{V'^2}{\omega_S^2} \tag{25}$$

The physical explanation for the increased instability is associated with the "S-like" shape of the velocity profile. As is well known from fluid dynamics this can drive the Kelvin-Helmholtz instability. To prevent the mode from being excited the Kadomtsev function, which characterizes the plasma properties, must be even more stabilizing than without flow. Thus, from the point of view of the plasma the velocity shear has led to a decrease in stability.

V. Cylindrical results

The goal of this section is to determine the effect of flow shear on the MHD marginal stability boundaries using the full cylindrical model with realistic LDX-like profiles. Achieving this goal requires a combination of cylindrical numerical studies and physical intuition based on the simple slab results of the previous section.

The starting point of the analysis is the specification of LDX-like equilibrium profiles. The pressure and density are chosen in accordance with expected experimental profiles as follows

$$\begin{aligned} p(r) &= p_w\left[\frac{(w+1)^\alpha}{w-1}\right]\left[\frac{x-1}{(x+1)^\alpha}\right] \\ \rho(r) &= \rho_{\max}\left(\frac{2}{1+x}\right) \end{aligned} \tag{26}$$

and are illustrated in Fig. 8a. Here $x=r^2/r_c^2$, $w=r_w^2/r_c^2$, and the plasma exists in the region $1\le x\le w$. For LDX $r_w=2m$ and the minor radius of the coil $r_c=0.15m$, implying that $w\approx 178$. The quantity p_w is the edge pressure, which is assumed to be held fixed by the wall properties during all simulations. The quantity α is a profile parameter that

determines how gradually the pressure profile decays to zero far from the coil. For a fixed edge pressure, high α implies a high peak pressure and a corresponding high value of β. The density decays as $\rho \propto 1/r^2$ at large distances and has the value $\rho = \rho_{\max}$ at the surface of the coil. The $1/r^2$ decay accounts for the fact that flux tubes can be randomly exchanged when the interchange mode is excited, usually near the outer portion of the plasma. Therefore, each flux tube must have the same number of particles implying that $\rho \propto 1/r^2$. In fact, Pastukhov and Chudin [23, 24] show that this scaling persists even during the nonlinear phase of the evolution of the interchange instability.

Next, note that the peak pressure occurs at $x_{\max} = (\alpha+1)/(\alpha-1)$ and is related to the edge pressure by

$$\frac{p_{\max}}{p_w} = \left[\frac{(\alpha-1)}{2\alpha}\right]^{\alpha-1}\left[\frac{(w+1)^{\alpha}}{\alpha(w-1)}\right] \tag{27}$$

To keep the number of free parameters manageable we assume that the plasmas of interest have low $p_{\max}$ and hence, low β. This is consistent with the experimental conditions on LDX and yields results that are very insensitive to the value of p_w except as it appears in simple scaling relations. The low β assumption enters the analysis by allowing us to accurately approximate the magnetic field by its vacuum value. Thus, the B_θ profile is given by

$$B_\theta(r) = \left(\frac{\mu_0 I_c}{2\pi r_c}\right)\frac{1}{x^{1/2}} \tag{28}$$

where I_c is the coil current.

The last profile of interest is that of the equilibrium flow velocity. In the analysis that follows two cases are considered:

$$V(r) = \frac{4V_{\max}}{(w-1)^2}(x-1)(w-x)$$
$$V(r) = \frac{V_{\max}}{(w^{1/2}-1)^2}\frac{(x-1)(w-x)}{x} \tag{29}$$

Both profiles satisfy the no slip condition as illustrated in Fig. 8b. The first profile reaches a maximum at $x_{\max} = (w+1)/2$, well beyond the pressure peak. Qualitatively, this profile might be generated by the $\mathbf{E}\times\mathbf{B}/B^2$ drift, which peaks far out because of the rapidly decreasing value of B. The second profile peaks at $x_{\max} = w^{1/2}$ which is much closer to the pressure maximum. Such a profile might be generated in a beam driven system. We emphasize that at present there is no detailed experimental data to motivate the choice of velocity profile and the two cases discussed should just be viewed as plausible possibilities.

The profiles have now been specified. The next step is to solve the cylindrical differential equation to determine the marginal stability boundary. In particular, in the low β limit we wish to determine the marginally stable value of the profile parameter α as a function of the maximum velocity $V_{\max}$. The strictest marginal α is determined by numerically searching for the marginal α at fixed k and $V_{\max}$, and then repeating the procedure by varying k until the lowest marginal α is found; that is, the strictest marginal α is defined as $\alpha(V_{\max}) = \min_k\left[\alpha_{mar}(k, V_{\max})\right]$. Knowing $\alpha(V_{\max})$ it is then straightforward to calculate the increase or decrease in critical β as a function of flow velocity. The critical figure of merit is defined as

$$\eta \equiv \frac{\beta_{\max}\left(V_{\max}\right)}{\beta_{\max}\left(V_{\max}=0\right)} \tag{30}$$

where

$$\begin{aligned}\beta &= \frac{2\mu_0}{B_\theta^2\left(r_w\right)}\left(\frac{2}{r_w^2-r_c^2}\int_{r_c}^{r_w} prdr\right)\\ &= \frac{8\pi^2 r_c^2}{\mu_0 I_c^2}\left(\frac{r_w^2}{r_w^2-r_c^2}\right)\int_1^w p\,dx\\ &\approx \frac{8\pi^2 r_c^2}{\mu_0 I_c^2}\int_1^\infty p\,dx\end{aligned} \tag{31}$$

and $\beta_{\max}$ is the largest value of β that is stable (the value corresponding to the marginal α). The last approximate expression corresponds to the interesting limit $w \gg 1$. For our profiles it follows that

$$\begin{aligned}\eta &= \left[\frac{\left(\alpha_0-1\right)\left(\alpha_0-2\right)}{\left(\alpha-1\right)\left(\alpha-2\right)}\right]\left\{\frac{1-\left[\left(\alpha-1\right)w-\left(\alpha-3\right)\right]/\left[2^{2-\alpha}\left(w+1\right)^{\alpha-1}\right]}{1-\left[\left(\alpha_0-1\right)w-\left(\alpha_0-3\right)\right]/\left[2^{2-\alpha_0}\left(w+1\right)^{\alpha_0-1}\right]}\right\}\left(\frac{w+1}{2}\right)^{\alpha-\alpha_0}\\ &\approx \left[\frac{\left(\alpha_0-1\right)\left(\alpha_0-2\right)}{\left(\alpha-1\right)\left(\alpha-2\right)}\right]\left(\frac{w}{2}\right)^{\alpha-\alpha_0}\end{aligned} \tag{32}$$

Here, $\alpha_0 = \alpha\left(V_{\max}=0\right)$ is the marginal value for zero flow and $\alpha = \alpha\left(V_{\max}\right)$ is the marginal value for finite flow. Observe that for $w \gg 1$ even a small increase in the marginal α due to flow can substantially increase the critical β since $\eta \propto w^{\alpha-\alpha_0}$.

The final preparatory step is to calculate the explicit conditions for marginal stability for the no-flow case $V_{\max}=0$. This will serve as the reference case when analyzing marginal stability for the two different velocity profiles. For $V_{\max}=0$, marginal stability in the cylindrical case occurs when $k \to \infty$ and requires that the Kadomtsev function be

positive for all r. In other words marginal stability occurs when $\min_r\left[K\left(r,\alpha_0\right)\right]=0$. For the profiles under consideration this condition reduces to

$$\min_x\left\{\frac{x\left[\left(\alpha_0+1\right)-\left(\alpha_0-1\right)x\right]}{\gamma\left(x^2-1\right)}+1\right\}=0 \tag{33}$$

The function in the brackets is plotted as a function of x in Fig. 9 and is labeled "K_0". Observe that the function is a monotonically decreasing function of x implying that the most unstable point is $x=w$. The marginal value of α for the reference case is thus given by

$$\alpha_0=\left(\frac{w+1}{w}\right)\gamma+\left(\frac{w+1}{w-1}\right)\approx\gamma+1 \tag{34}$$

For $\gamma=5/3$ and $w=\left(2/0.15\right)^2$ we find that $\alpha_0=2.687$.

We now turn to the cylindrical stability results for the two velocity profiles of interest.

A. First velocity profile

Some insight into the effect of the first velocity profile (the one that peaks far out) can be obtained by noting the following points. First, since $V''<0$ everywhere, there is no "S-like" behavior and the Kelvin-Helmholtz instability, as described by slab model (C), should not be excited. Second, over the major part of the profile the velocity shear is non-zero and in these regions, slab model (A) should apply, implying increased stability. Third, near the peak of the velocity, $V'=0$ by definition, and in this region slab model (B) should apply in which case there should be very little change in stability. Fourth, the marginal stability criteria for slab models (A) and (B) just happen to coincide when $V'=0$. The fifth and critical point is that when the velocity peaks far out (at

$x_{\max} \approx w/2$), the ratio of xp'/p is very nearly a constant over the entire region $x_{\max} < x < w$. Therefore, since xp'/p does not change, the marginal α obtained by setting $K(\alpha, x_{\max}) = 0$ is almost identical to the static value derived from $K_0(\alpha_0, w) = 0$.

The overall stability picture can be understood by examining the curve of $K_1(\alpha, S, x)$ vs. x also illustrated in Fig. 9. This curve corresponds to the local velocity shear stabilized Kadomtsev criterion given by Eq. (16), plotted for the case $\alpha = \alpha_0$ and $S = 1$. Here, S is an equivalent Mach number defined as a ratio of the maximum flow speed to the maximum sound speed of the static marginally stable plasma. The sound speed of the static plasma reaches it's maximum at $x = \alpha_0/(\alpha_0 - 2)$ and has the value

$$V_{S\max} = \sqrt{(\gamma p_{static}/\rho)_{\max}} = \left[\frac{\gamma p_w}{\rho_{\max}} \frac{(\alpha_0 - 2)^{\alpha_0 - 2}}{2^{\alpha_0 - 1}(\alpha_0 - 1)^{\alpha_0 - 1}} \frac{(w+1)^{\alpha_0}}{w-1}\right]^{1/2} \tag{35}$$

Thus, the parameter S is defined by

$$S = \left[\frac{V_{\max}^2}{V_{S\max}^2}\right]^{1/2} = \left[\frac{\rho_{\max} V_{\max}^2}{\gamma p_w}\right]^{1/2} \cdot \left[\frac{2^{\alpha_0 - 1}(\alpha_0 - 1)^{\alpha_0 - 1}}{(\alpha_0 - 2)^{\alpha_0 - 2}} \frac{w-1}{(w+1)^{\alpha_0}}\right]^{1/2} \tag{36}$$

Observe, that as expected $K_1 \geq K_0$, the equality occurring at the point $x_{\max} \approx w/2$ where $V' = 0$. Also, K_1 has a minimum very near $x = x_{\max}$. Technically, $K_1(\alpha_0, S, x_{\max})$ is greater than $K_0(\alpha_0, w) = 0$ implying that with flow, α can be raised above the value α_0 until marginal stability is reached: $K_1(\alpha, S, x_{\max)}) = K_0(\alpha_0, w) = 0$. However, because of the flatness of K_0, the gap $K_0(\alpha_0, w) - K_0(\alpha_0, x_{\max})$ is so small that the increase in α is virtually negligible.

The exact marginally stable α as a function of the velocity shear S, as predicted by the local slab model (A), is easily obtained by finding the value of $x = x_A$ that minimizes $K_1(\alpha, S, x)$:

$$\min_x \left\{ \frac{x\left[(\alpha+1)-(\alpha-1)x\right]}{\gamma\left(x^2-1\right)} + 1 + g_1 S^2 \left[\frac{x^2 (x+1)^{\alpha-1} (w+1-2x)^2}{(w-1)^4 (x-1)} \right] \right\} = 0$$
$$g_1(w) = \frac{12(\alpha_0-2)^{\alpha_0-2}}{2^{\alpha_0-1}(\alpha_0-1)^{\alpha_0-1}} \approx 1.192 \tag{37}$$

and then setting $K_1(\alpha, S, x_A) = 0$ to obtain $\alpha = \alpha(S)$. This curve is plotted in Fig. 10. Note that α increases with S as expected. Most of the increase occurs for small S as the minimum point of K_1 moves from the plasma edge, when $S = 0$, to its saturated value when the minimum coincides with the peak of the velocity. In any event the total increase is very small, raising α from 2.687 to 2.708. This produces a very modest gain in β given by $\eta = 1.05$.

The net result of this intuition is that the marginally stable values of α as predicted by slab models (A) and (B) are essentially identical and equal to the no-flow value α_0. The final conclusion is that the gain factor $\eta \approx 1$ (i.e. there is virtually no gain in β due to a sheared velocity flow that peaks far beyond the pressure maximum).

This intuition has been tested by numerically solving the full cylindrical eigenvalue equation for the profiles of interest using the LDX parameters and following the procedure described earlier. The results are similar to those just described. The peak of the eigenfunction moves from the plasma edge to the point where $V' = 0$ as S increases. The eigenfunction for large k is highly localized in space. The marginal α is very close

to α_0. Numerical inaccuracies associated with the use of finite rather than infinite k plus the high localization of the mode make it difficult to precisely calculate the very small differences in the marginal α as S varies. However, since the differences are very small it is not of great interest to pursue the numerical studies for the first velocity profile in any further detail.

B. Second velocity profile

Consider now the second velocity profile, which peaks much closer to the pressure maximum, at $x = x_{\max} = w^{1/2}$. This profile has a constant velocity shear over almost the entire region of unfavorable magnetic curvature and, consequently, we might expect to see an improvement in stability. This is indeed the case as can be intuitively understood by comparing the similarities and differences with respect to the first profile. The similarities are as follows. Again $V'' < 0$ everywhere so no Kelvin-Helmholtz instability is expected. Because of the large constant shear region, stability should be most similar to slab model (A). There is a small region close to the plasma where $V' = 0$ and in this region slab model (B) should apply. The stability criteria given by slab models (A) and (B) coincide in the region where $V' = 0$.

The critical difference is that the region where the criteria overlap is much closer to the peak pressure for the second velocity profile. In this region the ratio rp'/p is substantially different from its asymptotic value as $r \to \infty$. The implication is that at the overlap point the local stability criterion is satisfied by a substantial margin. Hence, we expect that it should be possible to raise α by a finite amount before reaching the marginal stability point.

This idea can be understood by examining the local stability curve corresponding to case (A) as a function of position. The curve is labeled $K_2 = K_2[\alpha, S, x]$ and is also illustrated in Fig.9 for the parameters $\alpha = \alpha_0, S = 1$. Observe that K_2 coincides with K_0 at the point where $V_2' = 0$ and has a minimum at $x = x_B$ slightly further out. It is clear from the curve that at this point $K_{2\min} = K_2(\alpha_0, S, x_B) > K_0(\alpha_0, w)$. Since raising α lowers curve K_2 when α is raised by a sufficient amount, then $K_2(\alpha, S, x_B) = K_0(\alpha_0, w) = 0$ and marginal stability has been achieved. The quantitative prediction of the marginal stability boundary $\alpha = \alpha(S)$ resulting from slab model (A) is easily obtained by solving

$$\min_x \left\{ \frac{x\left[(\alpha+1)-(\alpha-1)x\right]}{\gamma\left(x^2-1\right)} + 1 + g_2 S^2 \left[\frac{(x+1)^{\alpha-1}\left(w-x^2\right)^2}{\left(w^{1/2}-1\right)^4 x^2 (x-1)} \right] \right\} = 0$$
$$g_2(w) = \frac{3}{4} \frac{(\alpha_0-2)^{\alpha_0-2}}{2^{\alpha_0-1}(\alpha_0-1)^{\alpha_0-1}} \approx 7.45 \cdot 10^{-2} \tag{38}$$

The curve of $\alpha = \alpha(S)$ is illustrated as the solid curve in Fig. 11. We see that α increases with S and in the limit $S \to \infty$ saturates at the value 2.954 (for the given value of w). As a specific example, for $S = 1$ the marginal α has increased to 2.83, a substantial increase over the no flow limit. For this value of α the gain in β is finite: $\eta = 1.56$ The entire curve of η vs. S is shown as the solid curve in Fig. 12.

The overall insight from the slab analysis is that for velocity profiles peaked near the pressure maximum, the stabilizing effects of shear are substantial leading to finite increases in the marginally stable β.

This intuition has been tested by solving the cylindrical eigenvalue equation for the second velocity profile. Overall, the results are qualitatively similar although, as discussed shortly, there is one important effect that produces finite quantitative changes in the marginal stability boundary.

The first indication that shear provides a stabilizing effect is shown in Fig. 13 where we plot normalized growth rate $\omega_i / \left(V_{S\max} r_c \right)$ vs. S for the unstable case $kr_c = 1.5, \alpha = 2.95$ and $V_{S\max}$ given by Eq.(35). As has been found by several other authors [12, 13, 14], we see that the growth rate decreases as the velocity shear increases.

A second set of simulations illustrates normalized growth rate vs. wave number for various values of S at a fixed, unstable $\alpha = 2.95$ (See Fig. 14). Note that the growth rate decreases as the velocity shear increases. Interestingly, the fastest growth rates occur at very large kr_c. The growth rate initially increases with kr_c, then temporarily decreases and eventually starts to grow at large kr_c again. The explanation may lie in difference between the cylindrical and slab geometry. The interchange mode requires the highest possible wavenumber, while the plasma with velocity shear is most unstable for finite wavenumber. The competition between these two different effects is responsible for the behavior of the growthrate. This behavior has similarities with the growthrate observed by Guzdar et. al [16], where the competing effects were due to the KH and Rayleigh-Taylor modes.

The slab model also suggests that large kr_c should be completely stabilized by velocity shear above a critical value $\left(kr_c \right)_{crit}$ but this behavior is not observed in the cylindrical caseThe reason is again associated with finite cylindrical effects that spread

the eigenfunction over a larger portion of the profile when the plasma is unstable. The mode becomes localized only for large kr_c near marginal stability.

The difference in kr_c scaling relations between the slab and cylinder lead to quantitative changes in the marginal stability boundary for the following reason. Intuitively, we expect the slab model to be a reasonably accurate approximation to the cylinder when the modes are localized, which typically occurs for $kr_c \to \infty$. However, the slab model predicts that the most unstable wave numbers near marginal stability correspond to $kr_c \to 0$. This dichotomy can be seen by re-examining Fig. 11. Superimposed on the slab stability predictions are the cylindrical marginal stability results for various kr_c. For large kr_c the cylindrical and slab results are quite similar; as stated, in this regime the slab model is a good approximation. However, as kr_c decreases the marginal stability boundary is lowered (i.e. becomes more restrictive), finally reaching a saturated value when $kr_c \to 0$. For a given value of S the gain in α due to shear is approximately halved as kr_c decreases from infinity to zero. The gain in β due to velocity shear is also plotted in Fig. 12 for the actual cylindrical marginal stability boundary corresponding to $kr_c \to 0$. We see that the cylindrical β gain is more modest as compared to the slab prediction.

VI. Conclusions

The effect of velocity shear on the MHD interchange stability in a hardcore Z-pinch has been investigated in both slab and cylindrical geometries. The basic question is to determine whether velocity shear improves or worsens stability as compared to the static case. Our slab geometry results indicate that all options are possible, depending upon the

precise shape of the velocity profile. A constant velocity shear improves stability. A peaked velocity profile has little effect on stability. A counter-streaming S-shaped velocity profile worsens stability.

The slab results have been used to interpret numerical simulations of a cylindrical hardcore Z-pinch (modeling LDX) with a velocity profile corresponding to no-slip boundary conditions; i.e. the velocity is zero at each boundary and peaks in the middle. When the velocity profile peaks far from the pressure maximum, then the constant shear and peaked velocity criteria overlap. The net result is that there is almost no change in the marginal stability boundary due to the flow. On the other hand, when the velocity peaks near the pressure maximum, the constant shear slab model is the best approximation. There is a finite improvement in stability due to velocity shear, although quantitatively the cylindrical gains are more modest than the slab predictions.

Acknowledgements

The authors would like to thank Professor A. Hassam from University of Maryland for helpful discussions.

References:

1. Kesner, J., Bromberg, L., Garnier, D., Mauel, M., presented at 17th IAEA Conference of Plasma Physics and Controlled Nuclear Fusion, Yokohama, Japan 1998, paper IAEA-F1-CN-69/
2. D.T. Garnier, et al *"The Superconducting Levitated Dipole Experiment (LDX)", 15th Intl Toki Conference*, 12/2006, to be published in Fusion Engineering and Design (2006).
3. Kadomtsev B. B. (1966) in *"Reviews of Plasma Physics"*, edited by M. A. Leontovich, Consultants Bureau, New York, Vol. II.
4. I.B. Bernstein, E. Frieman, M. Kruskal and R. Kulsrud, (1958) Proc. Roy. Soc. A, 244, pp. 17-40.
5. J. Taylor, J. Nuclear Energy, Pt. C, 4, 406 (1962)
6. J.P. Freidberg and J.A. Wesson, Phys. Fluids **13**, 1117, (1970)
7. A. Bondeson, R. Iacono and A. Bhattacharjee, Phys. Fluids **30** pp. 2167-2180 (1987)
8. E. Hameri, Ph.D. thesis, New York University, 1976
9. E. Hameri and P. Laurence, J. Math. Phys. **25**, 396 (1984)
10. D. Garnier, J. Kesner and M. Mauel, Phys. Plasmas, vol. **6**, (1999) pp.3431-3434
11. A.N. Simakov, P. Catto, J. Ramos and R. Hastie, Phys. Plasmas, **9**, 4985 (2002).
12. V. Sotnikov et all, Phys. Plasma **9** (2002) pp.913-922
13. Y. Zhang and N. Ding, Phys. Plasmas **13**, (2006)
14. S. DeSouza-Macado et al., Phys. Plasma **7** (2000) pp. 4632-4643
15. H. Kuo, Phys. of Fluids, vol. **6**, p. 195 (1963)

16. P. Guzdar, P. Satyanarayana, J. Huba and S. Ossakow, Geophys. Research Lett., vol. **9**, p. 547 (1982)

17. A. Hassam, Phys Fluids B **4**,485 (1992)

18. A. Hassam, Phys. Plasmas (1999) pp. 3772-3777

19. A. Malagoli, G.Bodo and R. Rosner, The Astronomical Journal, 456, p. 708-716, (1996)

20. F. Brochard, E. Gravier and G. Bonhomme, Physics of Plasma, **12**, 062104 (2005)

21. E. Frieman and M. Rotenberg, Reviews of Modern Physics, vol. **32**, p.898 (1960)

22. A. Kouznetsov, Ph.D. thesis, Massachusetts Institute of Technology, 2007

23. V.P. Pastukhov and N.V.Chudin, Plasma Physics Reports, Vol. **27**, #11 (2001) pp. 907-921

24. V. P. Pastukhov and N. V. Chudin, 19th IAEA Fusion Energy Conf. Paper IAEA-TH/2-5, Lyon, France, 2003

List of Figures:

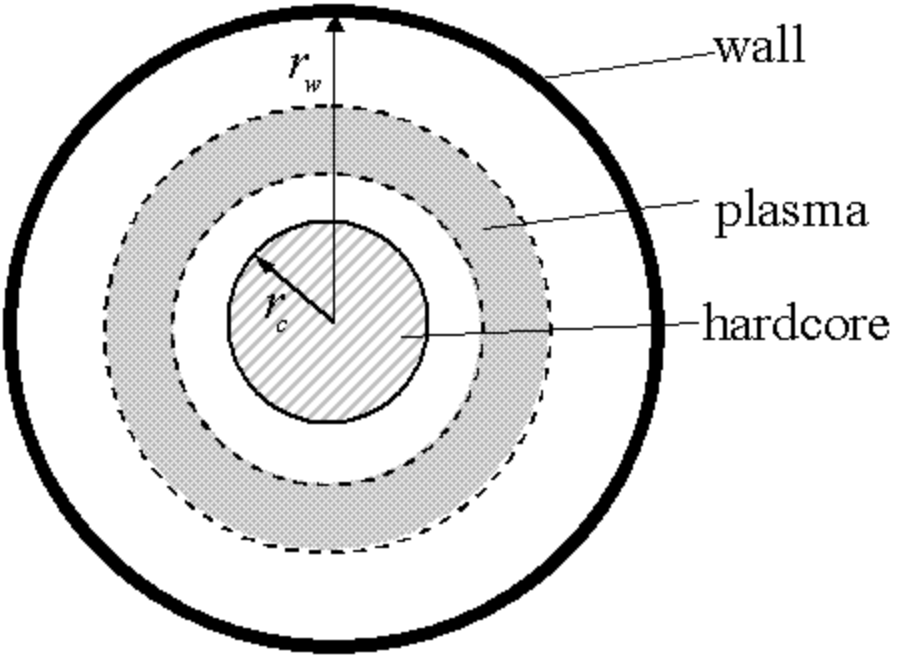
r_w
r_c
wall
plasma
hardcore

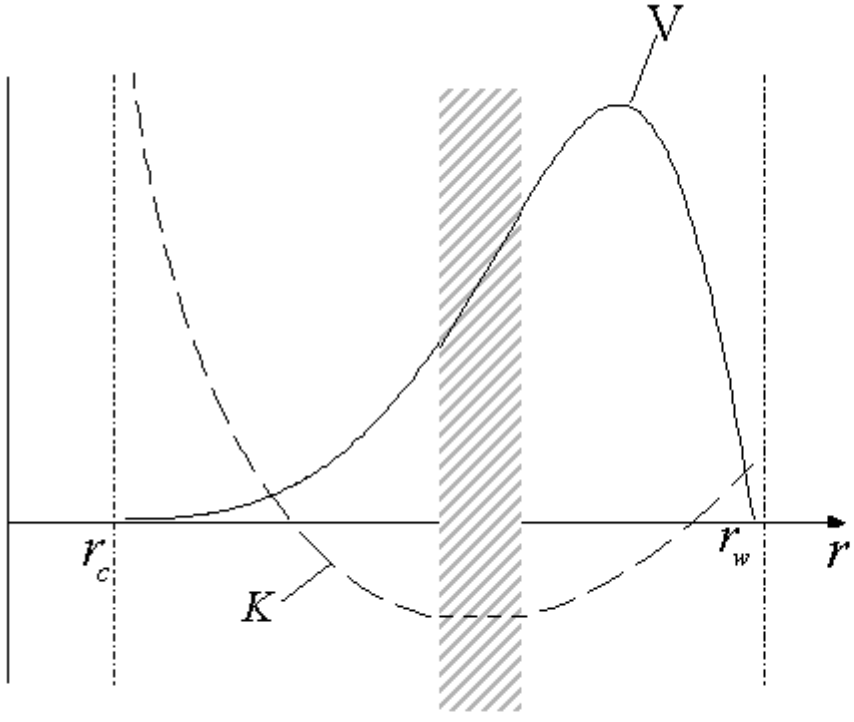

(a)

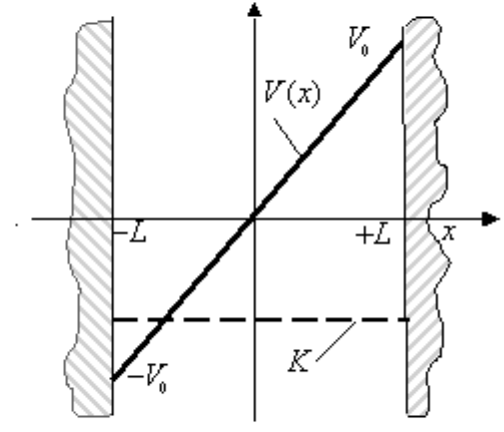

(b)

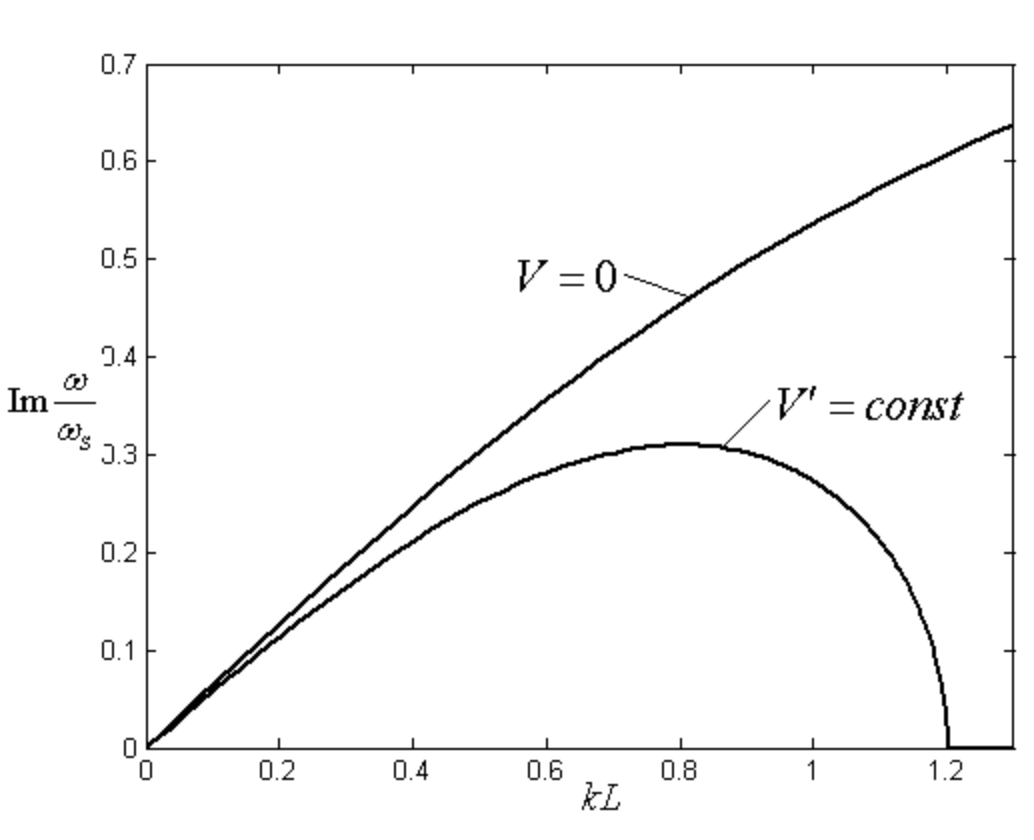
0.7
0.6
0.5
0.4
0.3
0.2
0.1
0
$\mathrm{Im}\frac{\omega}{\omega_s}$
$V = 0$
$V' = const$
0
0.2
0.4
0.6
0.8
1
1.2
kL

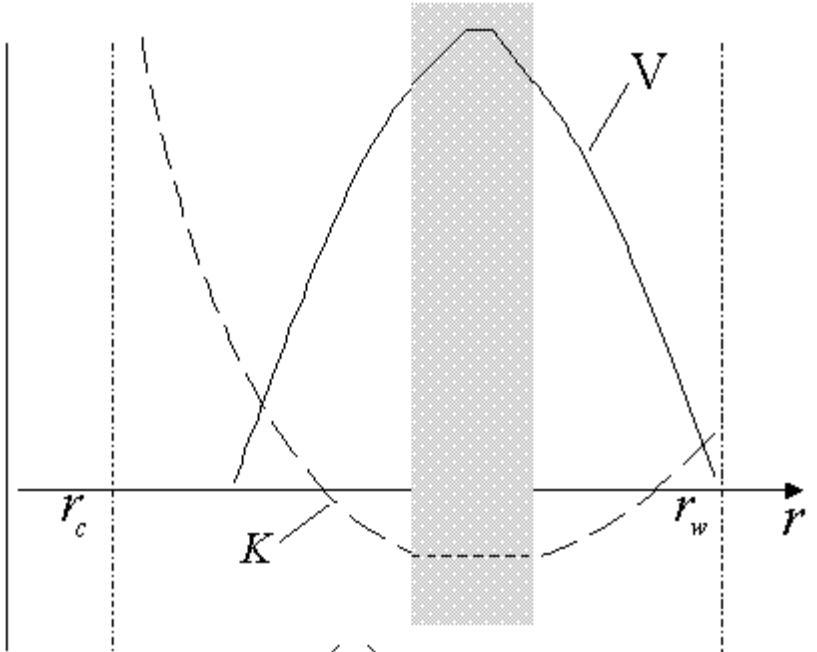

(a)

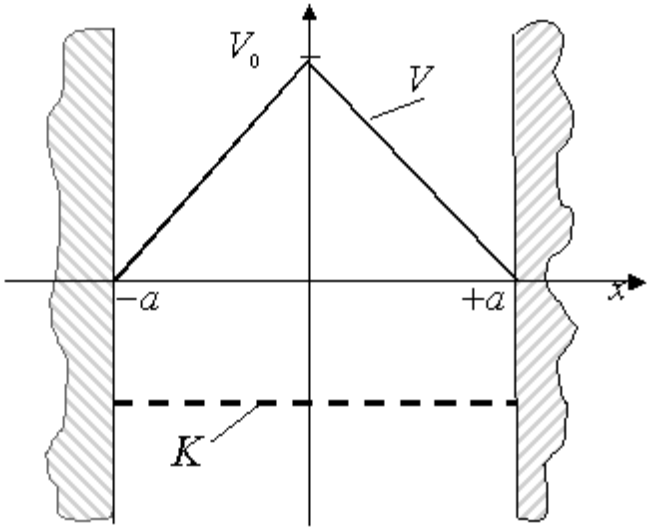

(b)

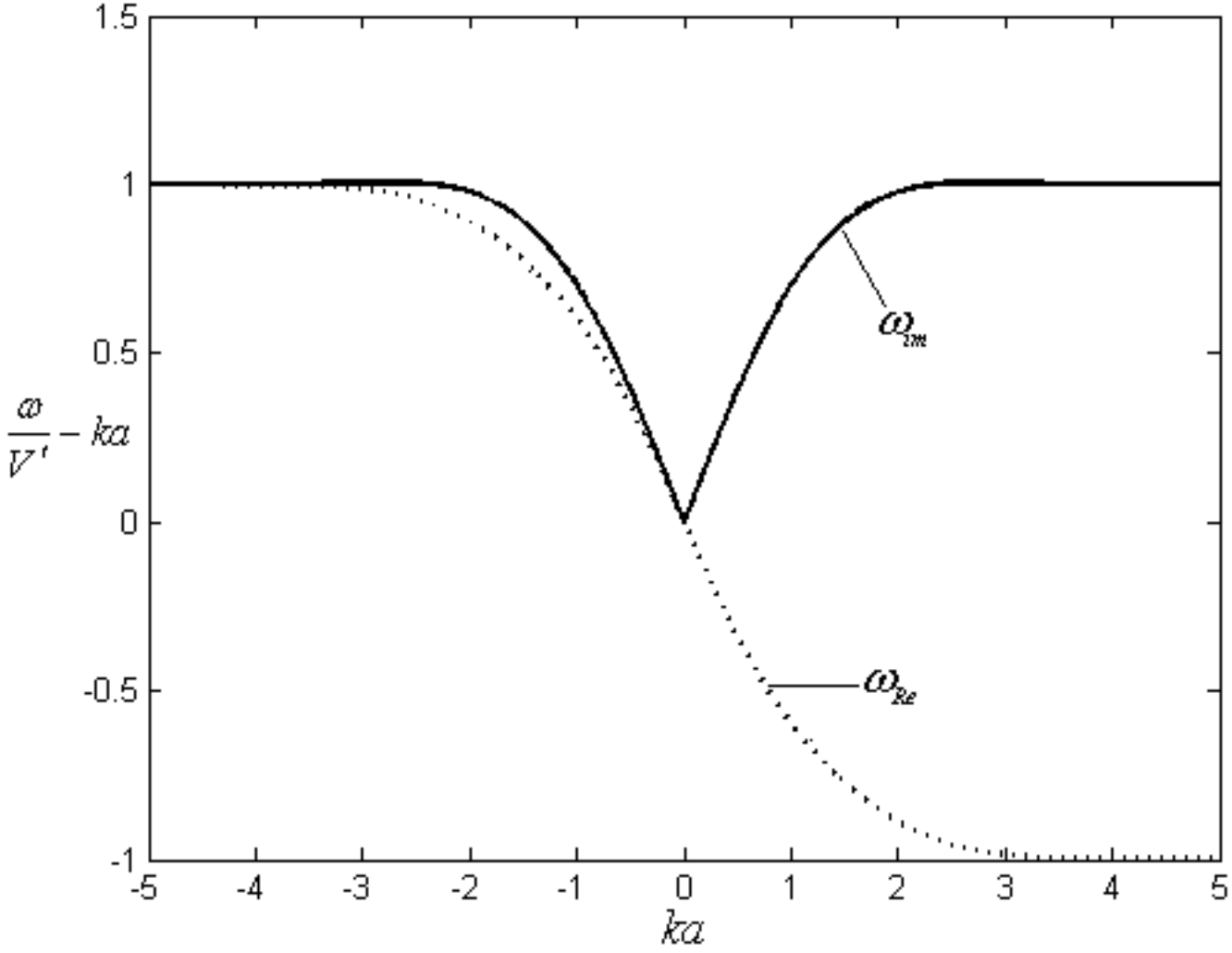
1.5
1
0.5
0
-0.5
-1
-5
-4
-3
-2
-1
0
1
2
3
4
5
$\frac{\omega}{V'} - ka$
ka
ω_{im}
ω_{Re}

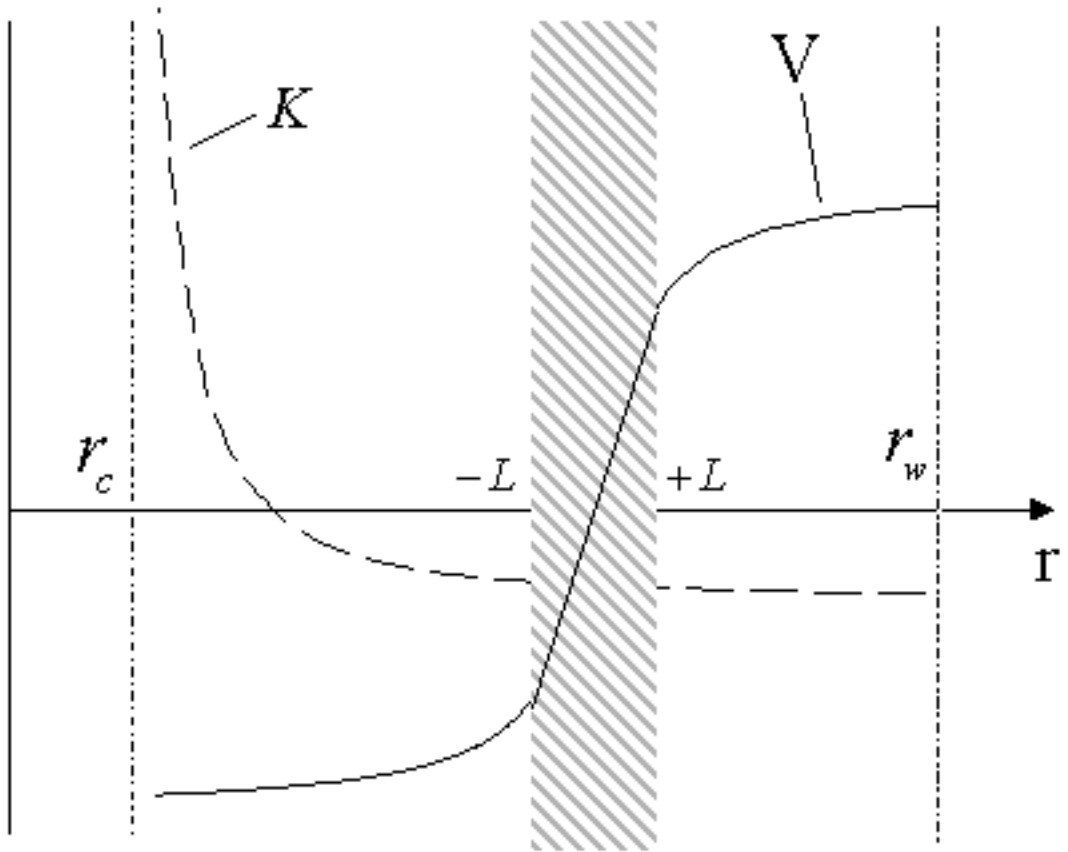

(a)

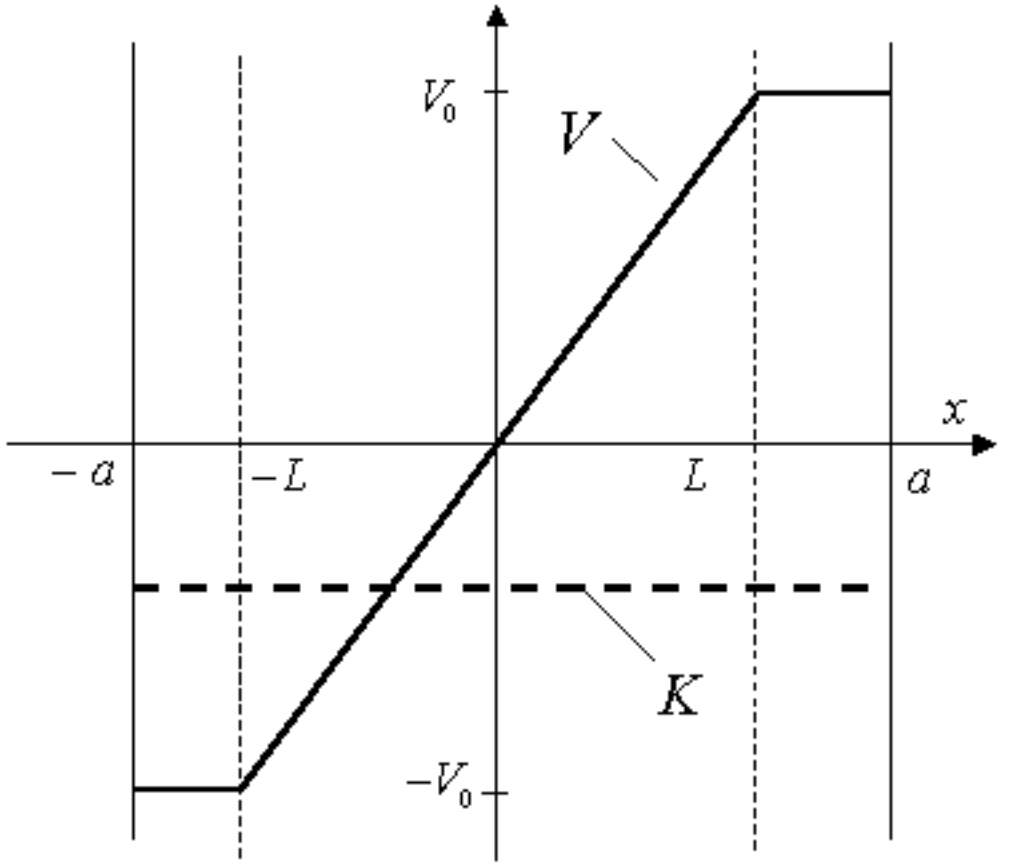

(b)

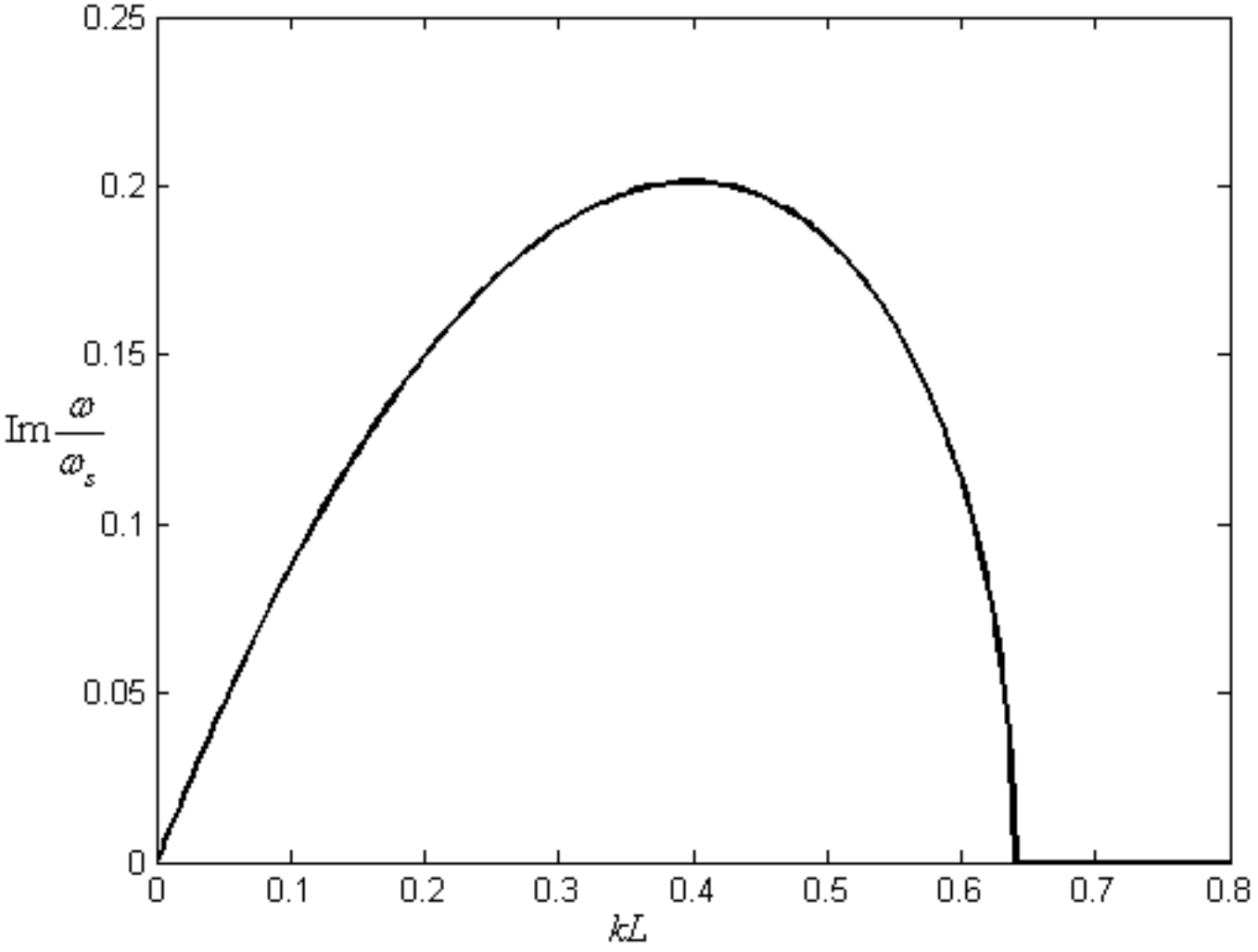
0.25
0.2
0.15
0.1
0.05
0
Im $\frac{\omega}{\omega_s}$
0
0.1
0.2
0.3
0.4
0.5
0.6
0.7
0.8
kL

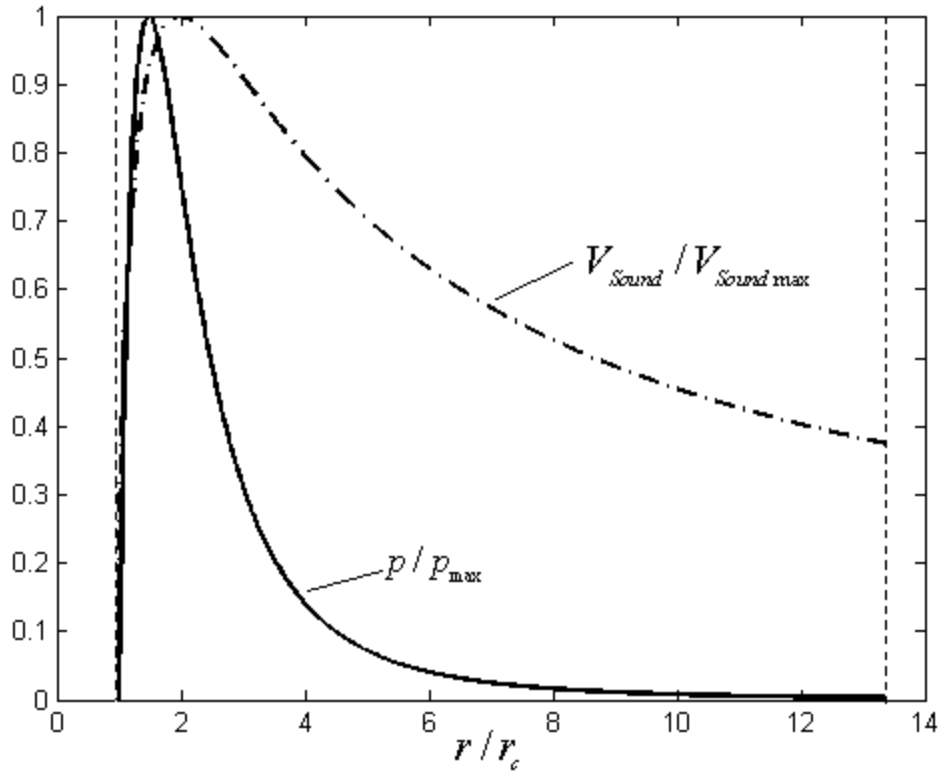
1
0.9
0.8
0.7
0.6
0.5
0.4
0.3
0.2
0.1
0
0
2
4
6
8
10
12
14
$V_{Sound} / V_{Sound\,max}$
p / p_{max}
r / r_c

(a)

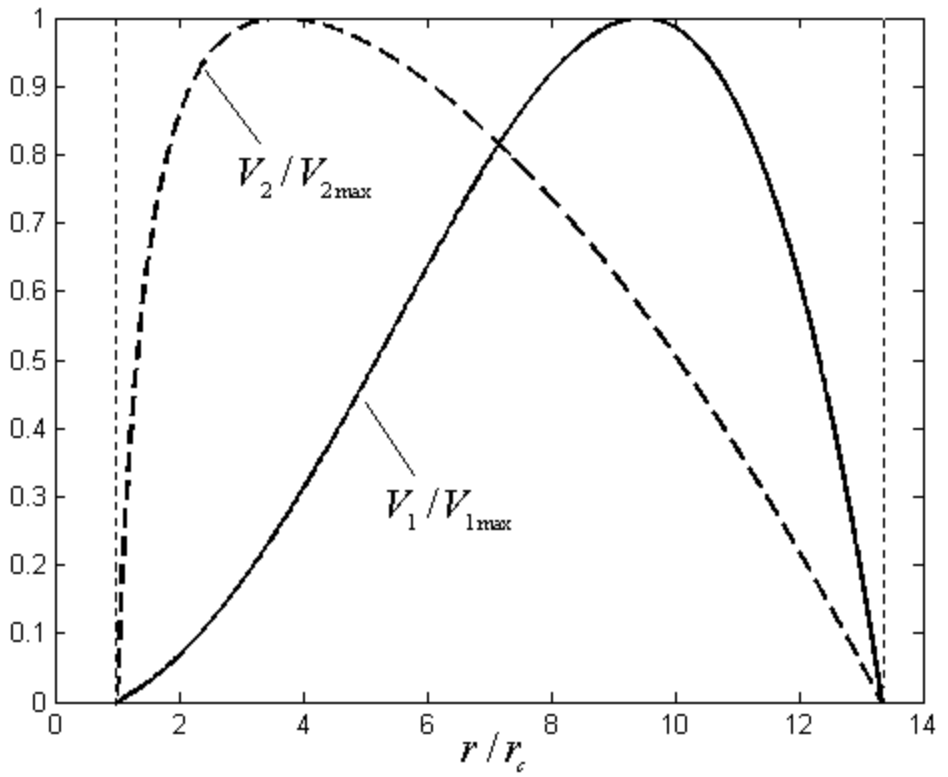
1
0.9
0.8
0.7
0.6
0.5
0.4
0.3
0.2
0.1
0
0
2
4
6
8
10
12
14
V_2 / V_{2max}
V_1 / V_{1max}
r / r_c

(b)

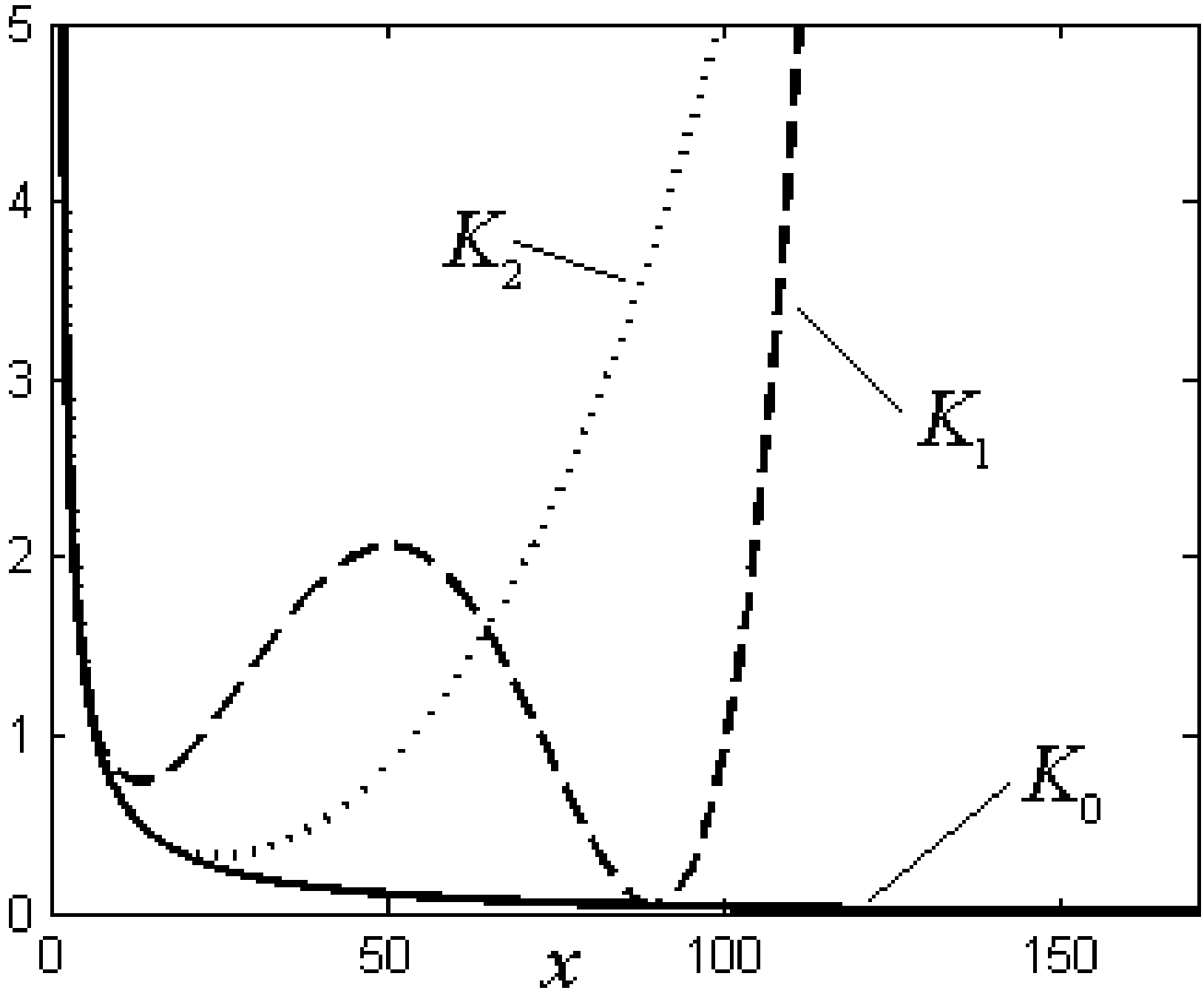
5
4
3
2
1
0
0
50
100
150
x
K_2
K_1
K_0

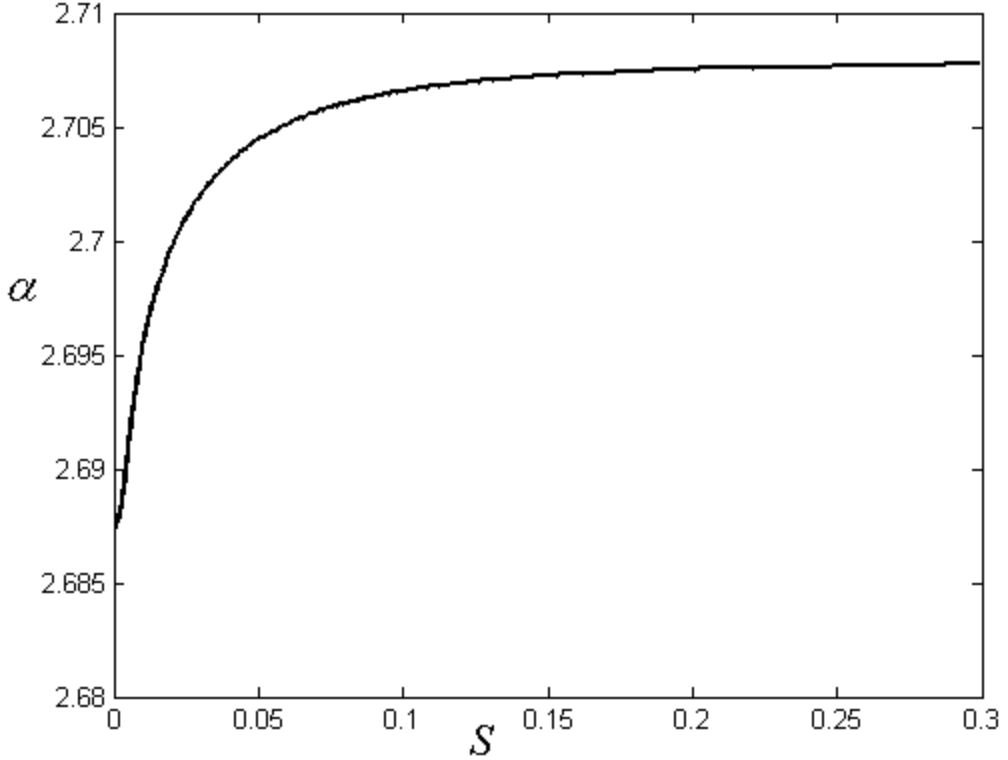
2.71
2.705
2.7
2.695
2.69
2.685
2.68
α
0
0.05
0.1
0.15
0.2
0.25
0.3
S

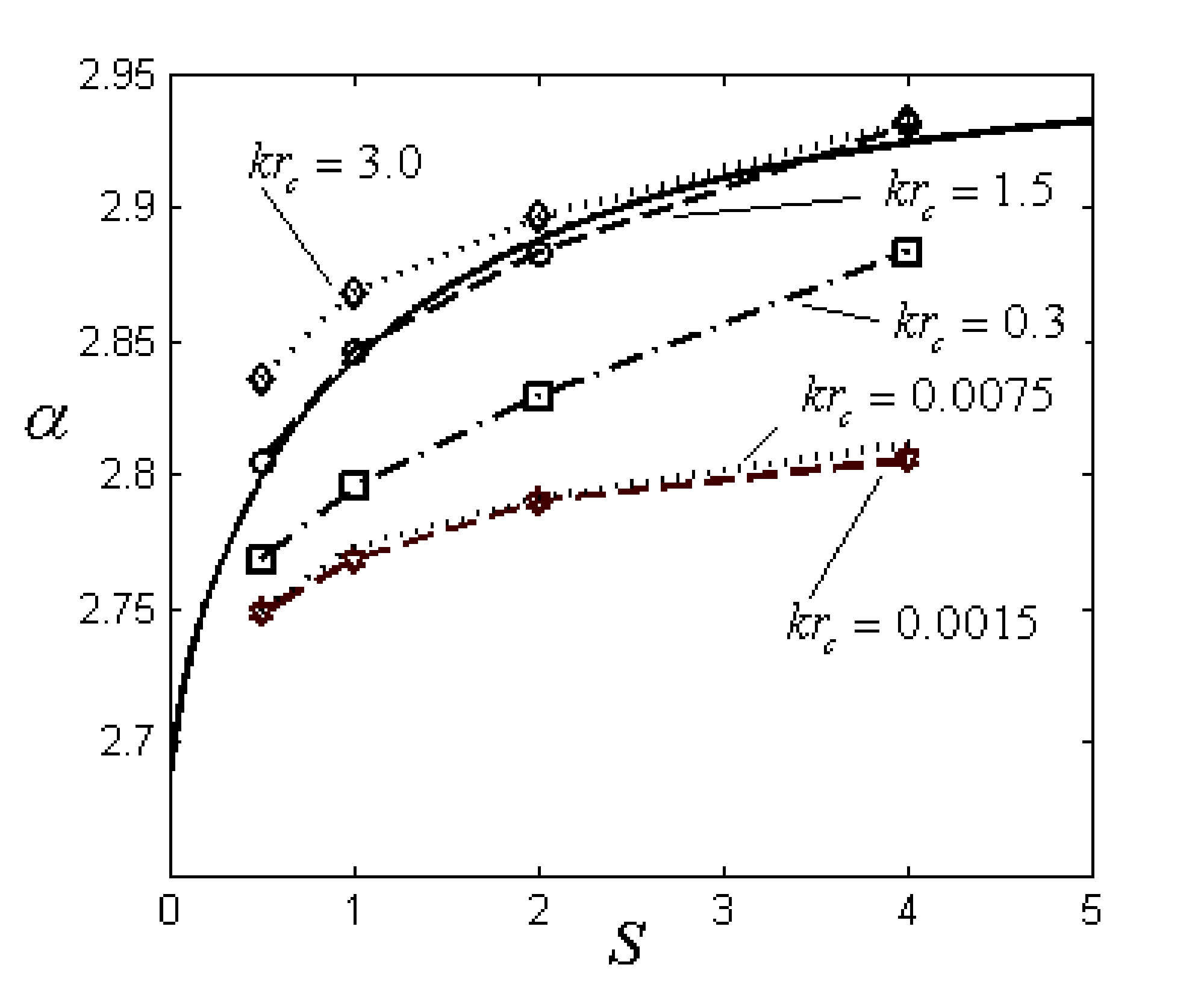
2.95
2.9
2.85
2.8
2.75
2.7
α
0
1
2
3
4
5
S
$kr_c = 3.0$
$kr_c = 1.5$
$kr_c = 0.3$
$kr_c = 0.0075$
$kr_c = 0.0015$

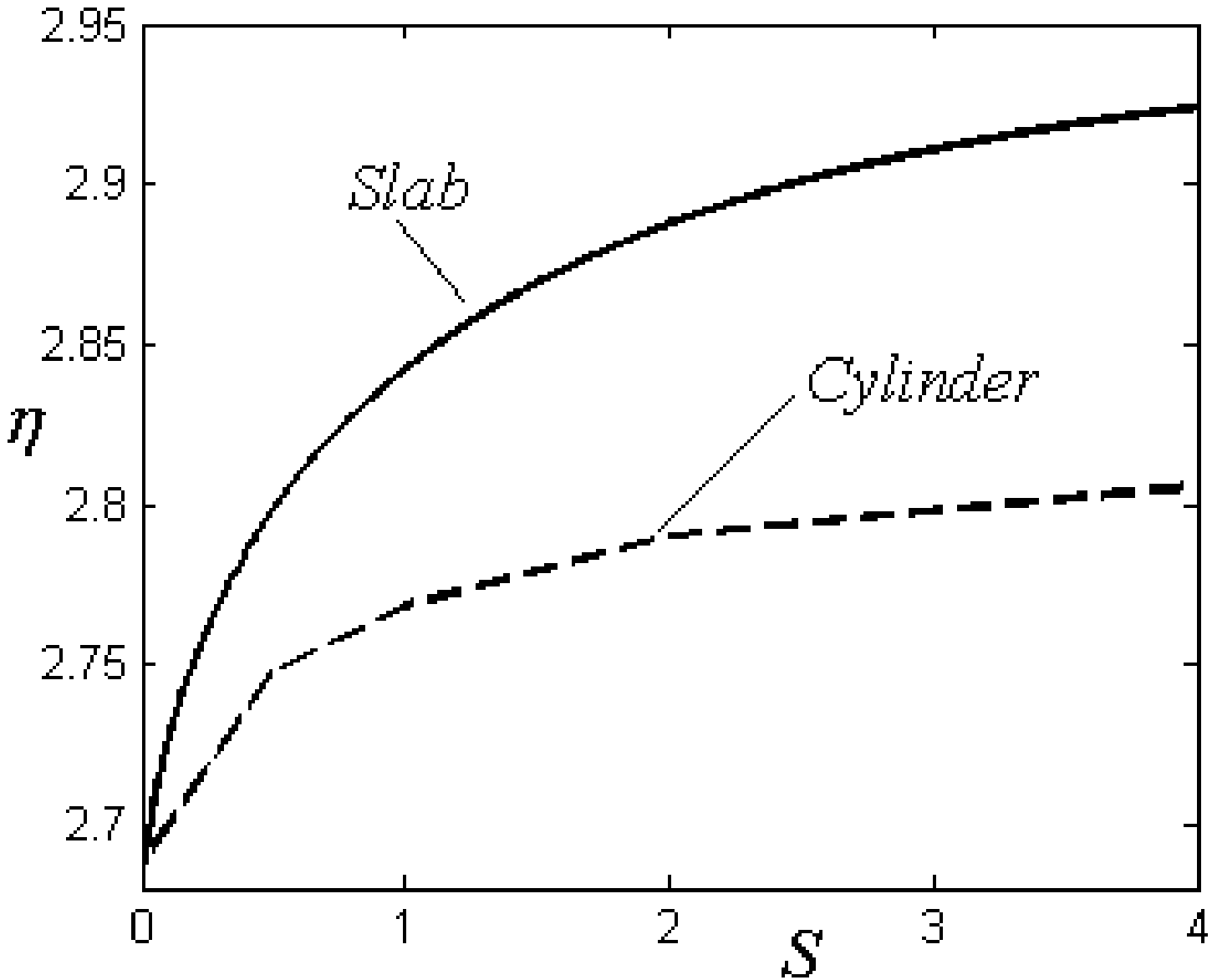
2.95
2.9
2.85
2.8
2.75
2.7
η
Slab
Cylinder
0
1
2
3
4
S

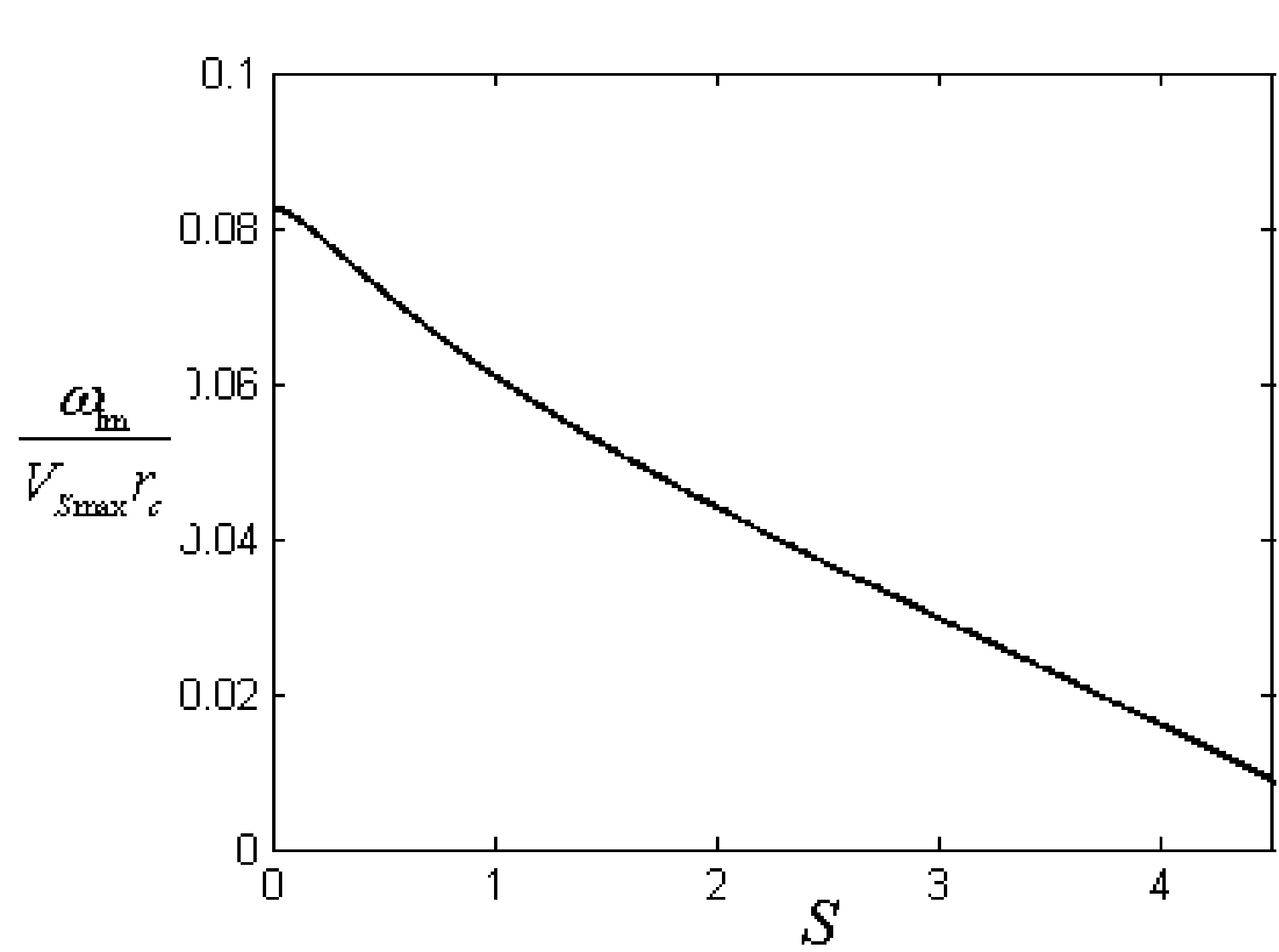
0.1
0.08
0.06
0.04
0.02
0
0
1
2
3
4
S
$\frac{\omega_{hm}}{V_{Smax} r_c}$

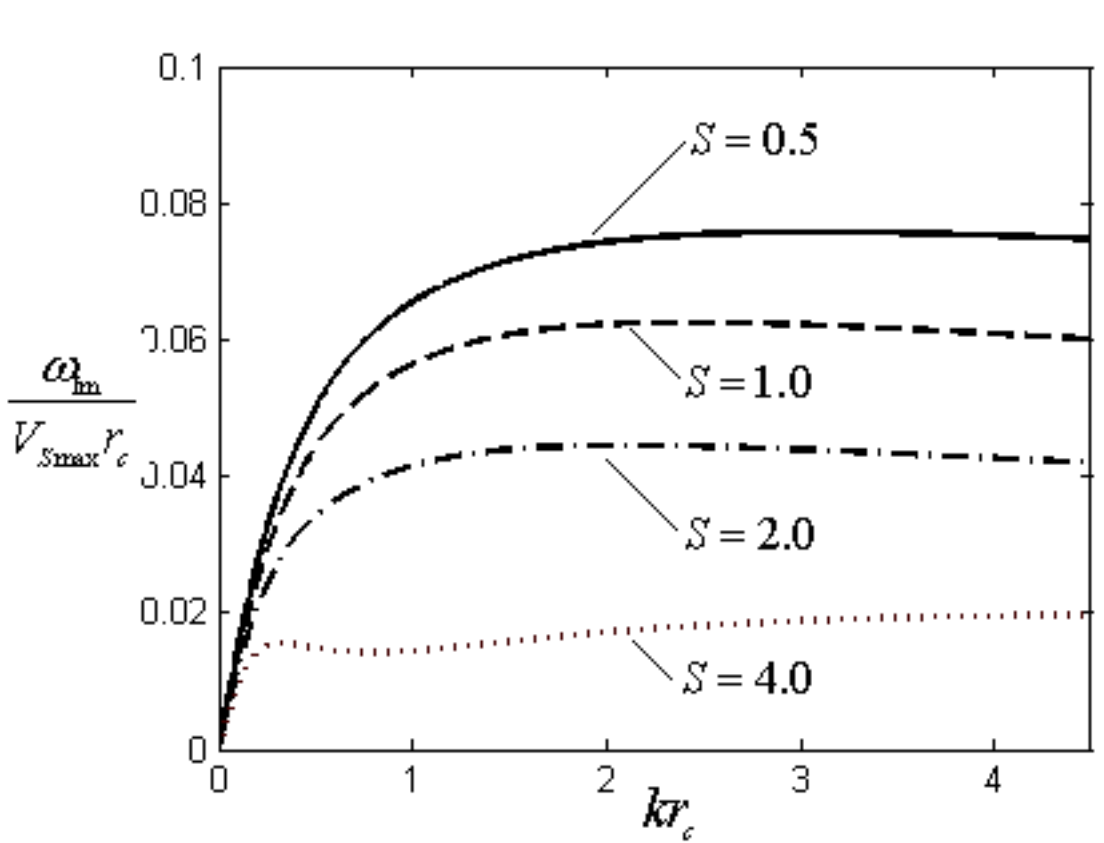
0.1
0.08
0.06
0.04
0.02
0
0
1
2
3
4
$\frac{\omega_{bn}}{V_{S\max} r_c}$
kr_c
$S = 0.5$
$S = 1.0$
$S = 2.0$
$S = 4.0$